Micromachines **2014**, *5*, 216-227; doi:10.3390/mi5020216

OPEN ACCESS

micromachines

ISSN 2072-666X

www.mdpi.com/journal/micromachines

Article

Biomimetic *Pieris rapae*'s Nanostructure and Its Use as a Simple Sucrose Sensor

David Bonzon [1,*], Rodrigo Martinez-Duarte [2], Philippe Renaud [1] and Marc Madou [3]

[1] Laboratoire de Microsystèmes LMIS4, Ecole Polytechnique Fédérale de Lausanne, Station 17, CH-1015 Lausanne, Switzerland; E-Mail: philippe.renaud@epfl.ch

[2] Mechanical Engineering Department, Clemson University, 250 Fluor Daniel, Clemson, SC 29634, USA; E-Mails: rodrigm@clemson.edu

[3] Mechanical and Aerospace Engineering Department, University of California Irvine, 4200 Engineering Gateway, Irvine, CA 92617, USA; E-Mail: mmadou@uci.edu

***** Author to whom correspondence should be addressed; E-Mail: david.bonzon@epfl.ch; Tel.: +41-21-69-36582.

Received: 25 March 2014; in revised form: 11 April 2014 / Accepted: 14 April 2014 / Published: 23 April 2014

Abstract: Biomimetics often provides efficient ways to create a product incorporating novel properties. Here we present the replication of the *Pieris rapae* butterfly optical structure. This butterfly has white wings with black spots. The white coloration is produced by light scattering on pterin beads ranging from 100 to 500 nm whereas black spots correspond to areas without pterin beads, thus revealing a highly pigmented layer underneath. In order to mimic the butterfly wing structure, we deposited SU-8 beads produced by electrospraying on a black absorbing layer made of black SU-8. We thereby replicated the optical effect observed on *Pieris rapae.* Additional experiments showed that the white coloration replication is a structural color. Finally, we further demonstrate that these optical engineered surfaces can be used for sucrose sensing in the range of 1 g/L to 250 g/L.

Keywords: biomimetic; *Pieris rapae*; electrospraying; SU-8; mie scattering; refractive index sensing

---

1. Introduction

In biomimetics we observe nature and try to replicate it to provide efficient ways to produce man-made products often incorporating novel properties. Numerous examples of this can be found in micro and nano systems. An interesting case was the demonstration of the self-cleaning of certain plants' surface by Bartholl *et al.* [1] who demonstrated how the nano-structures on these plants' cuticle make them super hydrophobic. From this initial observation, different artificial replicas were produced and super hydrophobic surfaces were successfully demonstrated for human applications. One example of such an application was presented by Zorba *et al.* [2] who, using laser machining, produced silicon surfaces of controlled roughness. In a well-known somewhat older example of biomimetics, De Mestral [3] created a hook and loop fastening device commercialized under the brand name Velcro®, inspired by the observation of burrs sticking to his dog's fur. Along the same line, more recently Gorb *et al.* [4] presented another adhesive microstructure inspired by a beetle's attachment system based on a mushroom-shaped fibrillar adhesive. In this case, the combination of the contact splitting, high aspect ratio and spatula-shaped heads of the structure provides a strong adhesion.

In optics, the bright colors exhibited by butterflies are often not caused by dyes but by interference or scattering of light on patterned/structured surfaces and are part of an intense field of study to paint by alternative means, *i.e.*, by patterning surfaces that like a butterfly's wing, give rise to structural colors [5]. A particular example in this general area is the case of the Blue Morpho butterfly whose blue iridescent color comes from a natural Bragg reflector formed by stacked layers of cuticle and air [6]. The Blue Morpho butterfly example has led to multiple biomimetic approaches using different types of microfabrication including techniques such as PDMS soft lithography [7] and nano-imprinting technique [8].

In this study we focus on the *Pieris rapae* butterfly that has white wings with black spots (Figure 1). Previous work by Stavenga *et al.* [9] revealed the presence of pterin beads ranging in size from 100 nm to 500 nm in the white areas and found that the black spots on the wings are lacking those beads. Additionally, the same researchers also demonstrated that the wetting of the butterfly's wings in a solvent with a refractive index close to that of the beads leads to a darker appearance of the wing. Morehouse *et al.* [10] have suggested that the white coloration is due to light scattering on the afore mentioned pterin beads and according to Giraldo *et al.* [11] the black coloration is caused by a high concentration of pigments in the underneath layers coupled with the absence of beads.

The goal of this work was to replicate the optical structure of the *Pieris rapae* butterfly wings. A black absorbing layer was used to replicate the black coloration and polymer beads to replicate the white coloration. The polymer beads were deposited using electrospraying of SU-8 on a black absorbing layer produced by a pyrolized spin-coated 2 μm thick film of SU-8 process. We have demonstrated that the obtained white coloration is structural in nature according to the Mie scattering theory [12]. Finally, we further demonstrate that these optical engineered surfaces can be used for refractive index sensing through an application of sucrose sensing in the range of 1 g/L to 250 g/L.

Figure 1. (**a**) *Pieris rapae* butterfly with white wings and black spots; (**b**) SEM pictures of *Pieris rapae* butterfly microstructure showing white areas of the wings that correspond to the areas populated with beads; (**c**) SEM pictures of *Pieris rapae* butterfly microstructure showing black areas of the wings that correspond to the areas where beads are missing.

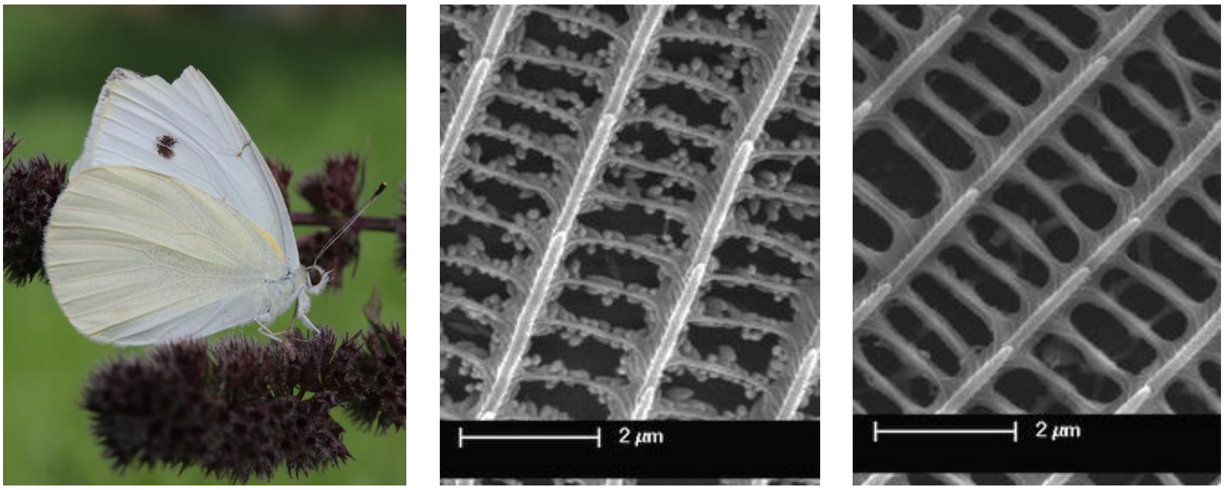

(**a**) (**b**) (**c**)

2. Materials and Methods

Processes for the *Pieris rapae* butterfly wing color replication are detailed below with a first section describing the black layer fabrication and a second section describing the replication of the beads used as Mie scatterers as well as their size evaluation. The method for the light scattering measurements is presented in a fourth section.

2.1. Black Layer Fabrication

A black absorbing layer was produced by spin-coating 2 μm of carbon-black SU-8 (I-37, Gersteltec, Pully, Switzerland) on a silicon wafer (Si wafers 100/P/SS/01-100, CMI-EPFL, Lausanne, Switzerland). Spin coating parameters were set at an acceleration of 100 rpm/s to reach a constant speed of 1000 rpm that was maintained for 40 s (LMS200, Sawatec, Sennwald, Switzerland). The wafer was then baked for 3 min at 120 °C and 20 min at 220 °C with a temperature ramp rate of 5 °C/min (HP401Z, Sawatec, Sennwald, Switzerland). Measured layer thickness was 2.12 μm and measured mean roughness (Ra RMS) was 498 Å (Alpha-Step 500, Tencor, San Jose, CA, USA). SU-8 layer was subsequently pyrolized to increase substrate conductivity allowing charges evacuation to keep a low substrate potential facilitating the electrospraying deposition. The pyrolysis was performed using an ATV PEO-600 furnace with a ramp of 10 °C/min to reach a first step at 250 °C maintained for 30 min and a second step at 900 °C maintained for 75 min. Nitrogen gas was flowed in the furnace with a flow-rate of 1000 L/h.

2.2. Fabrication of Mie Scatterers

To replicate the Mie scatterers present on the *Pieris rapae*'s wings we used dielectric beads made of SU-8. The beads were produced using an in house-built electrospraying setup as shown in Figure 2.

The following protocol was developed to produce beads as suggested by Steach *et al.* [13] with a size distribution comprised between 100 and 500 nm as found on the *Pieris rapae* butterfly. According to Sharma *et al.* [14] low viscosity polymers solutions (SU-8 2002 and 2005 from Microchem, Newton, MA, USA) were used to produce the beads. The polymer solution was dispensed from 23 and 27 gauge needles (2) connected to a high voltage supply (3) (HV350R, Information Unlimited, Mont Vernon, NH, USA) capable of generating DC voltages of up to 20 kV. The black substrate (1) described in the previous section was placed in front of the needle orifice with a calibrated distance and was used to collect the electrosprayed material. A syringe pump (4) (PHD 2000, Harvard Apparatus, Holliston, MA, USA) was used to impose a constant flowrate during the electrospraying process. Specific parameters found for the beads replication are given in the results section. In the electrospraying process, SU-8 beads are dried during their flight but no further polymerization step such as curing was performed.

Figure 2. Electrospraying setup used to deposit SU-8 beads on the black absorbing substrate (**1**). It is composed of a spraying needle (**2**) set at a DC voltage controlled by a high voltage supply (**3**) and the polymer is injected through the needle using a syringe pump (**4**).

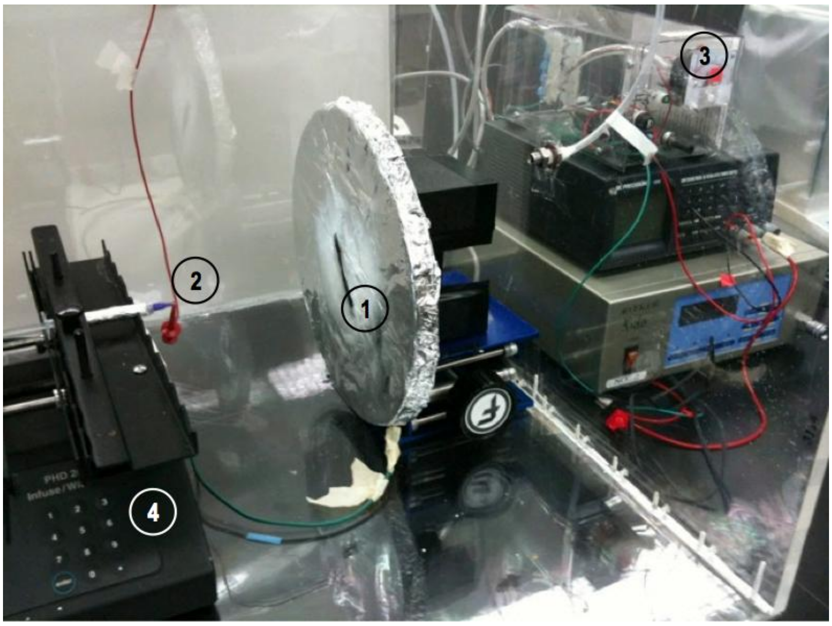

2.3. Beads Size Evaluation

Images of deposited beads were acquired by scanning electron microscopy (Quanta 23 FEG, FEI, Hillsboro, OR, USA) with an acceleration voltage of 10 kV without any conductive coating. An area of $3 \times 3\ \mu m^2$ comprising an amount of beads ranging from a few tens to a few hundreds of beads was acquired. Image J was used to determine the number of beads and their size. The average size value and its corresponding standard deviation were subsequently extracted from the analysis of at least 20 beads.

2.4. Scattered Light Measurements

The light scattered from the electrosprayed SU8 beads was measured using reflectance spectroscopy. Our in house-built set-up is shown in Figure 3. The excitation comes from a cold light halogen lamp (Haloid Lamp 150 W, AmScope, Irvine, CA, USA) and is focused on the sample using a converging lens with a focal length of 7.5 cm. The light scattered from the sample is collected using a fiber collimator positioned at a 20° angle with respect to the axis defined by the illumination and the converging lens (as presented in the schematic diagram in Figure 3). The scattering light spectrum is measured with a spectrophotometer (USB4000, Ocean Optics, Dunedin, FL, USA). The reflected light spectrum used as a reference consists of the light spectrum scattered by a piece of PTFE. In the last results section, the measurement of scattered light for refractive index evaluation is performed at 600 nm. This wavelength was chosen as it corresponds to a red LED excitation, which is potentially an inexpensive excitation solution.

Figure 3. (**a**) Schematic and (**b**) picture of the in-house built setup used to characterize the light scattered from the beaded surface.

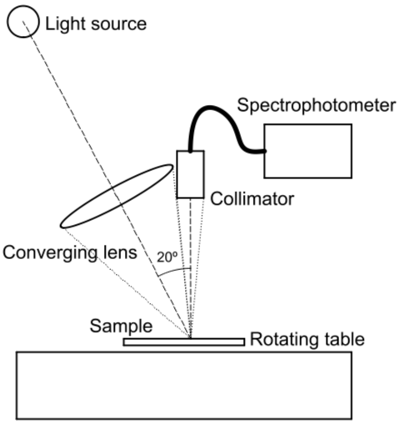

(**a**)

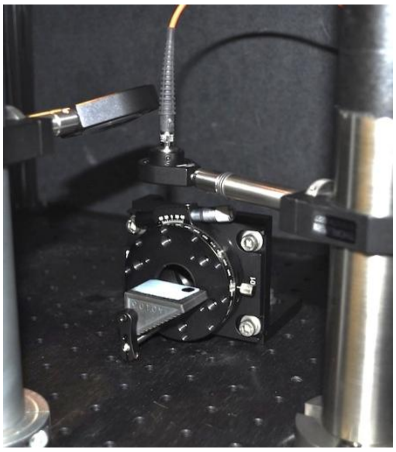

(**b**)

3. Results and Discussion

3.1. Beads Fabrication & Coloration Replication

To tune the beads size, several parameters have been optimized; polymer viscosities, voltages, flow-rates and distances between the needle and the substrate. Figure 4 illustrates the effect of those four parameters on the average size of the beads and on the size distribution given by their average value and standard deviation (error bar) respectively. To elucidate the effect of these parameters and to discern underlying trends, measurements at the extreme of each parameter setting were carried out. With trends established, a fine-tuning of those four parameters was performed in order to reach the 100 to 500 nm beads size as found with the butterfly. According to these experiments, an increase of polymer viscosity tends to increase the beads size but also increase the bead size distribution. Moreover, our experiments confirmed that only low viscosity polymer solutions produce beads as previously shown by Sharma *et al.* [14]. As a consequence this parameter does not present a lot of flexibility for beads size tuning. An increase of the syringe pump flow-rate increases beads size but also increases its distribution rapidly and above 0.6 mL/h beads are not clearly separated from each other anymore. Additionally, we observed that changing the distance between the needle and the substrate has only a minor effect on the bead size as this setting influences simultaneously two parameters that have an opposite effect on the bead size: the electric field and the time of flight. Finally, an increase of the applied voltage decreases the bead size and we found this parameter to be the most efficient for bead size tuning and established that it is possible to produce polymer beads with a size ranging between 100 and 500 nm as found on the *Pieris rapae* butterfly using SU-8 2002, a voltage of 12 kV, a distance of 8 cm and a flow-rate of 0.25 mL/h.

Figure 4. Evolution of the beads average size and distribution (standard deviation of the bead size shown in the error bar) according to the change of the electrospraying parameters such as the polymer viscosity, syringe pump flow-rate, voltage and distance between the needle and the substrate. (**a**) Variation of the viscosity between SU-8 2002 and SU-8 2005. Other parameters were a voltage of 12 kV, a distance of 8 cm, a gauge 27 needle and a flow-rate of 0.08 mL/h; (**b**) variations in the flow-rate from 0.3 to 0.9 mL/h. Other parameters were a voltage of 20 kV, a distance of 10 cm, a gauge 23 needle and SU-8 2005 was used; (**c**) variations in the voltage between 12 and 18 kV Other parameters were a distance of 8 cm, a flow-rate of 0.08 mL/h, a gauge 27 needle and SU-8 2002 was used; (**d**) variations in the distance needle-substrate between 8 and 12 cm. Other parameters were a voltage of 12 kV, a flow-rate of 0.08 mL/h, a gauge 27 needle and the SU-8 2002 was used. It is shown that the voltage is an efficient parameter to tailor the bead size while parameters such as distance between electrodes tend to show weaker effect.

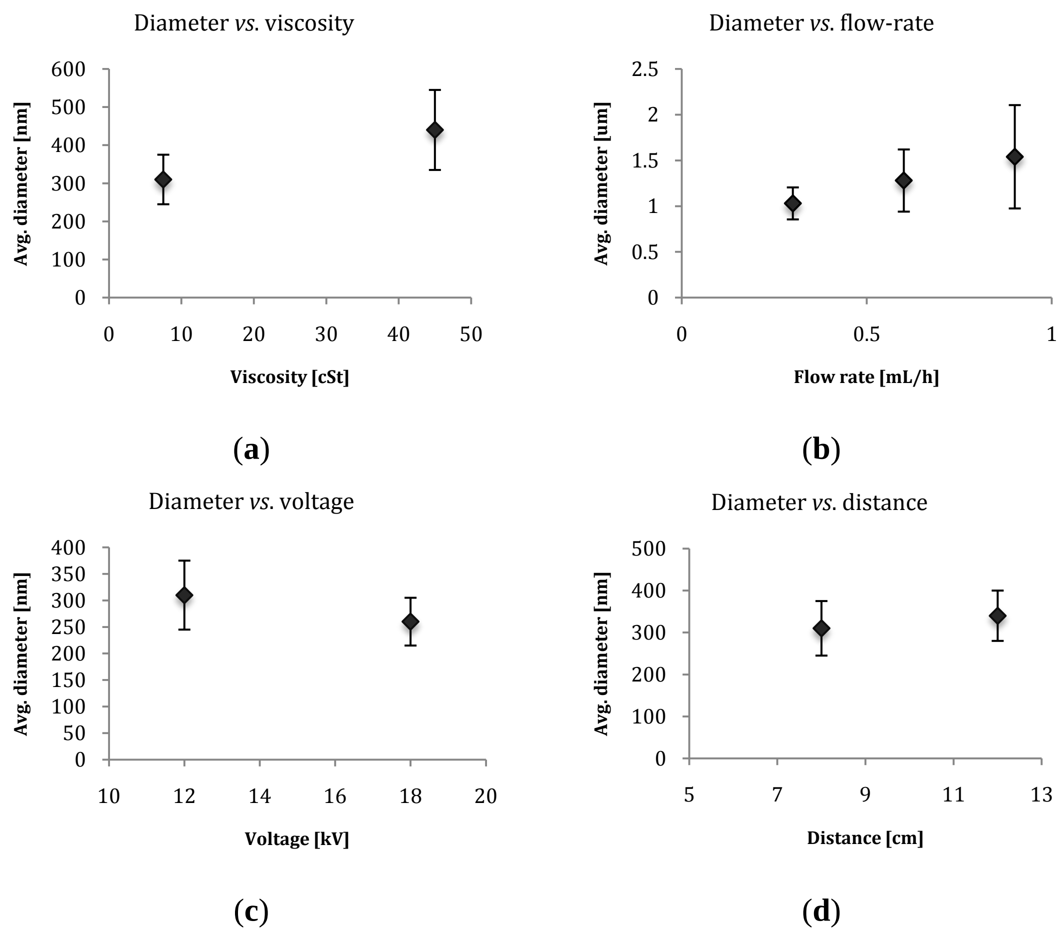

In order to replicate the coloration pattern of the *Pieris rapae* butterfly, shadow masks were used to selectively deposit scatterers according to the butterfly color pattern (see Figure 5). Two different masks and different spraying times were used to generate the two different gray tones patterns replicating the butterfly color pattern as faithful as possible (see Figure 6). The spraying time for the darkest gray tone was 2 min 50 s and the cumulative spraying time for the lightest area was 5 min 10 s.

Figure 5. (**a**) Layer diagram of the butterfly wings replication showing dielectric (SU-8) beads sprayed through a shadow mask onto a silicon wafer previously coated with black SU-8 (I-37, Gersteltec, Pully, Switzerland) that was pyrolyzed to facilitate the bead deposition using electrospraying; (**b**) SEM picture of dielectric (SU-8) beads in the range of 100 to 500 nm produced by electrospraying to mimic Mie scatterers found on the *Pieris rapae* butterfly.

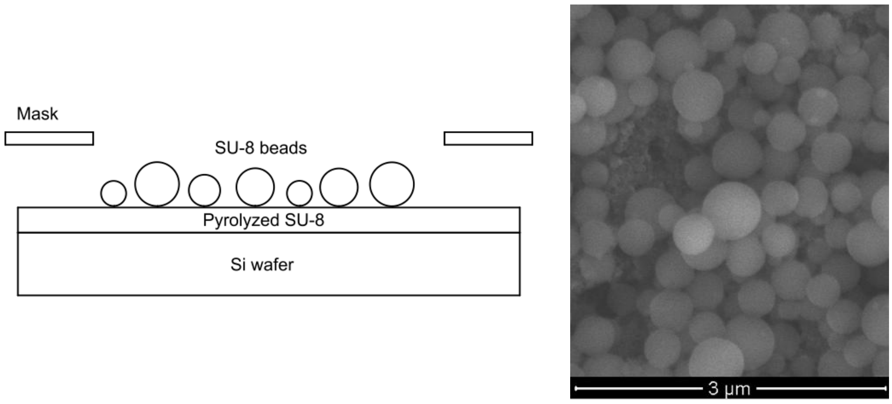

(a) (b)

Thereby, dielectric beads of a diameter in the range of 100 to 500 nm as found in the *Pieris rapae*'s wings have been successfully reproduced using electrospraying of SU-8. Figure 6 shows the result of the sprayed beads on a black SU-8 absorbing layer. We observe that the white coloration of the *Pieris rapae* butterfly has been reproduced using artificial produced SU-8 beads. Grey tones were also obtained at the edges of the wings by varying the beads density using a two-steps spraying process through different shadow masks as described above.

Figure 6. (**a**) Actual *Pieris rapae* butterfly wings showing white coloration with black spots; (**b**) result of *Pieris rapae* replication: the white surface is produced by SU-8 beads with diameters in the range of 100 to 500 nm. Black dots are the result of the black pyrolyzed layer without beads.

(**a**) (**b**)

3.2. Proof of the Structural nature of the Color Obtained

To demonstrate that we are dealing with structural white color and not a dye we performed reflectance measurement with the produced nanostructured surface. As demonstrated in Figure 7, the wetting of the replicated surface with DI water decreased the reflectance dramatically something that one does not expect when covering a surface coated with a dye. In the case of the dry surface, an almost flat curve is observed over the whole visible wavelength range as expected from its white appearance and similarly to the real butterfly reflectance spectrum showing a plateau between 450 and 700 nm [9]. In the case of the DI water wetted surface, the reflected light is decreased as the refractive index of the medium surrounding the beads is shifted now from 1.0 to 1.333 edging toward the SU-8 refractive index of 1.67. These results are in agreement with the Mie scattering model [12] and give evidences for the structural based white coloration.

Figure 7. (**a**) Reflectance spectrum of the *Pieris rapae* butterfly replica in the case of a dry and wetted surface with DI water; (**b**) picture of the surface with a dry and a wet circular area qualitatively showing the same effect of light scattering decrease due to the wet condition.

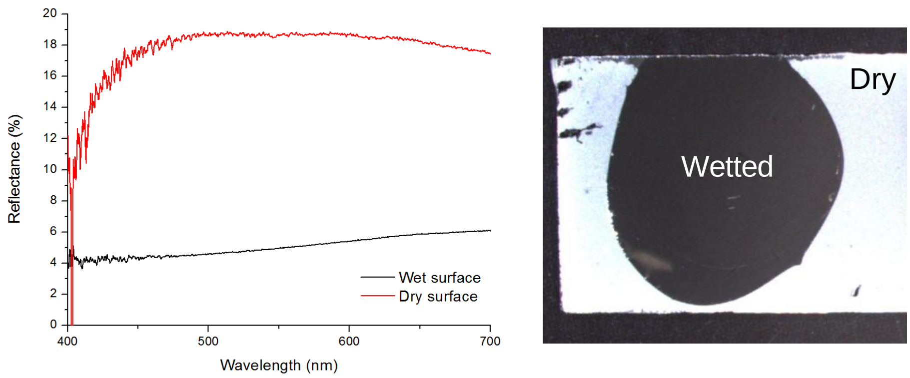

(**a**) (**b**)

3.3. Sucrose Sensing Application

The previous experiment demonstrated that the refractive index surrounding the beads determines the intensity of the scattered light. Hence, it suggests the possibility to use such a structured surface for measuring the refractive index of an unknown medium through the reflected light coming from such a structure. The black surface patterned with polymeric beads presented above was thus tested as a possible sucrose sensor.

The refractive index of sucrose solutions is known to depend on the sucrose content and has been measured to vary between 1.333 for pure water to 1.450 for solution containing 700 g of sucrose per liter [15]. According to van de Hulst [12], the Mie scattering obtained in the case of spheres depends on the refractive index of the surrounding medium. The closer the indexes of the medium and of the spheres, the smaller the scattering. Figure 8 illustrates the light reflectance from the artificial butterfly wing structure wetted with different sucrose concentrations. As the sucrose concentration increases from 0 to 250 g/L its refractive index also increases from 1.333 to 1.36 and the scattering of light is reduced. This graph shows that the sucrose concentration can be directly measured by evaluating the light scattering intensity on the artificial butterfly wing structure.

Figure 8. Evolution of the reflectance of the butterfly wing replica when covered by a sucrose solution of increasing concentration. The reflectance was measured at 600 nm.

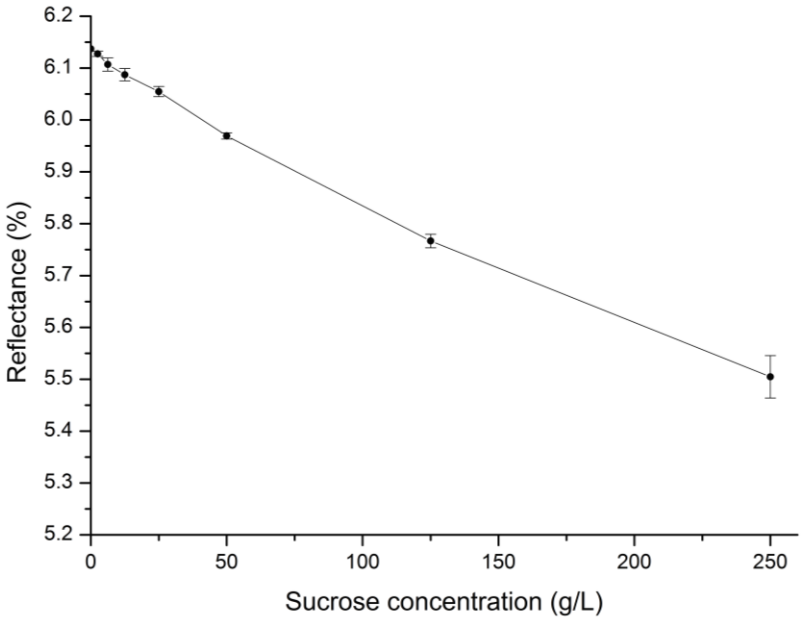

3.4. Discussion

Although the *Pieris rapae* butterfly wing and our replica exhibit a similar white appearance, the artificial butterfly micro structure does differ substantially from the actual wing structure. Importantly, on the actual *Pieris rapae* butterfly wing, the beads are attached to a periodic rectangular structure as shown in Figure 1b. Also, the pterin beads in the actual butterfly wing are not touching the surface but are suspended on those rectangular frames. The rectangular bead suspending frames could have a photonic crystal effect and consequently some specific wavelengths could be attenuated. Those bead suspending rectangular structures were not reproduced in the current study. Making an identical *Pieris rapae* structure with electrospraying alone would be hard but could be manufactured using a combination of photolithography and electrospraying. Given the reflectance results obtained in this study without the rectangular structures and with beads directly touching the substate, we believe that effects related to photonic bad gaps or Bragg filter effects are small compared to the effect of the diffusive bead structures. In other words, the dominant effect is the Mie scattering of the randomly organized SU-8 beads. Resonances for specific frequencies given by the bead size and refractive index are cancelled out by the dispersion in bead size, which explains the white spectra obtained both in the replica and the actual butterfly. The effect of the suspending rectangular structures in the butterfly wing could be to minimize the interaction between the substrate and the beads to possibly strengthen the light scattering. This might explain the brighter coloration of the butterfly's wings compared to that of our replica. In order to mimic such structures, other beads fabrication methods were presented in the literature with an example of Scholz *et al.* [16] synthesizing ZnS nanospheres by homogeneous precipitation. This alternative method has the particularity to produce monodispersed spheres; hence scattering exhibits resonance at specific wavelength.

The replicated beaded structure was also used to make a sucrose sensor. In this case, scattered light from the surface is modulated by the refractive index of the medium surrounding the beads. Hence, increasing sucrose concentration leads to a measurable decrease in scattered light. This refractive index sensor is very easily produced and could be made very inexpensively but its sensitivity is at least one order of magnitude lower than that of a plasmonic-based refractive index sensor. However, our technique seems appropriate to sense sucrose in the range starting from 1 g/L up to the limit of sucrose dissolution in water. This range coincides with the amount of sucrose present in pre-fermented wine must or beer wort. Indeed our technique offers a resolution close to the one of the winemaker portable refractometer (~1 g/L) while presenting the same drawback, which is its lack of specificity. Therefore, this technique could be an alternative to the refractometer used in that industry, which is expensive due to optical components used, such as prisms, and fragile due to optical coating required.

4. Conclusions

In this work, the *Pieris rapae* butterfly coloration pattern was successfully replicated using a scalable and low-cost electrospraying method. A protocol to create SU-8 dielectric beads was established and the effects of electrospraying parameters such as voltage, polymer viscosity, distance between needle and collector as well as flow-rate on bead size and bead size distribution were evaluated and discussed. After parameters tailoring, dielectric SU-8 beads in the range of 100 to 500 nm—the same as found in the actual *Pieris rapae*—were produced and these beads were shown to generate the same light scattering as the pterin beads in the butterfly. We argue and give evidence that the coloration mechanism of the replica is mostly structural. The manufacturing process introduced here is easy to set up and highly scalable and we suggest it can be used to obtain large diffusive surfaces.

Finally, as another application of the beaded surfaces produced by electrospraying we show that these surfaces can also be used for refractive index sensing. In this regard a sucrose sensor is demonstrated. This suggests the possibility of using such low cost and easy to fabricate structures as refractive index sensors with a possible application for sucrose detection in the winemaking industry.

Acknowledgments

We would like to acknowledge Sébastien Jiguet from Gersteltec Sàrl for kindly providing the black SU-8 as well as support for the spincoating and pyrolysis processes.

We also acknowledge UCI BioMEMS and EPFL LMIS4 group members for their help and support during this work.

Author Contributions

David Bonzon designed and conducted experiments, fabricated the butterfly replication and wrote the manuscript. Rodrigo Martinez Duarte contributed to the butterfly replication fabrication and reviewed the manuscript. Philippe Renaud co-supervised the work and reviewed the manuscript.

Marc Madou gave the original idea of this research, contributed to the design of experiments, supervised the work and contributed to the writing of the manuscript.

Conflicts of Interest

The authors declare no conflict of interest.

References

1. Barthlott, W.; Neinhuis, C. Purity of the sacred lotus, or escape from contamination in biological surfaces. *Planta* **1997**, *202*, 1–8.
2. Zorba, V.; Stratakis, E.; Barberoglou, M.; Spanakis, E.; Tzanetakis, P.; Anastasiadis, S.H.; Fotakis, C. Biomimetic artificial surfaces quantitatively reproduce the water repellency of a lotus leaf. *Adv. Mater.* **2008**, *20*, 4049–4054.
3. De Mestral, G. Separable Fastening Device. US Patent 3,009,235, 21 November 1961.
4. Gorb, S.; Varenberg, M.; Peressadko, A.; Tuma, J. Biomimetic mushroom-shaped fibrillar adhesive microstructure. *J. R. Soc. Interface* **2007**, *4*, 271–275.
5. Biró, L.P.; Vigneron, J.P. Photonic nanoarchitectures in butterflies and beetles: Valuable sources for bioinspiration. *Laser Photon. Rev.* **2011**, *5*, 27–51.
6. Vukusic, P.; Sambles, J.R. Photonic structures in biology. *Nature* **2003**, *424*, 852–855.
7. Kang, S.-H.; Tai, T.-Y.; Fang, T.-H. Replication of butterfly wing microstructures using molding lithography. *Curr. Appl. Phys.* **2010**, *10*, 625–630.
8. Saito, A.; Miyamura, Y.; Ishikawa, Y.; Murase, J.; Akai-Kasaya, M.; Kuwahara, Y. Reproduction, Mass Production, and Control of the Morpho Butterfly's Blue. In *Proc. SPIE 7205, Advanced Fabrication Technologies for Micro/Nano Optics and Photonics II*; SPIE: Bellingham, WA, USA, 2009; Volume 7205.
9. Stavenga, D.G.; Stowe, S.; Siebke, K.; Zeil, J.; Arikawa, K. Butterfly wing colours: Scale beads make white pierid wings brighter. *Proc. Biol. Sci.* **2004**, *271*, 1577–1584.
10. Morehouse, N.I.; Vukusic, P.; Rutowski, R. Pterin pigment granules are responsible for both broadband light scattering and wavelength selective absorption in the wing scales of pierid butterflies. *Proc. Biol. Sci.* **2007**, *274*, 359–366.
11. Giraldo, M.A.; Stavenga, D.G. Sexual dichroism and pigment localization in the wing scales of pieris rapae butterflies. *Proc. Biol. Sci.* **2007**, *274*, 97–102.
12. Van de Hulst, H.C. *Light Scattering by Small Particles*; Dover Publications: New York, NY, USA, 1981.
13. Steach, J.K.; Clark, J.E.; OIesik, S.V. Optimization of electrospinning an SU-8 negative photoresist to create patterned carbon nanofibers and nanobeads. *J. Appl. Polym. Sci.* **2009**, *118*, 405–412.
14. Sharma, C.S.; Vasita, R.; Upadhyay, D.K.; Sharma, A.; Katti, D.S.; Venkataraghavan, R. Photoresist derived electrospun carbon nanofibers with tunable morphology and surface properties. *Ind. Eng. Chem. Res.* **2010**, *49*, 2731–2739.
15. Yunus, W.M.M.; Rahman, A.A. Refractive index of solutions at high concentrations. *Appl. Opt.* **1988**, *27*, 3341–3343.

16. Scholz, S.M.; Vacassy, R.; Dutta, J.; Hofmann, H.; Akinc, M. Mie scattering effects from monodispersed ZnS nanospheres. *J. Appl. Phys.* **1998**, *83*, 7860–7866.